Research Article

Table 1. Baseline viral and host characteristics among genotype-1b null responders and their virologic outcome.

Patient	*IL28B* GT	HCV RNA, $\log_{10}$ IU/ml	NS5A polymorphism(s)[a]	NS3 polymorphism(s)[a]	Virologic outcome
P-1	CT	7.2	Q54H/Q-Q62Q/E-Y93H/Y	T54S-Q80L	SVR
P-2	CT	7.0		Q80L-V170I/M	SVR
P-3	CT	7.4	Q54H		SVR
P-4	CT	6.7	R30Q		SVR
P-5	CT	7.0	L31L/M-P58P/S		SVR
P-6	CC	5.3	P58P/T-Q62E		D/C at Wk2 due to SAE[b]
P-7	CC	7.2		S122S/G	SVR
P-8	CT	7.0	Q54H	Q80L	SVR
P-9	CT	7.1	Q54H-Y93H/Y	S122N	SVR
P-10	CT	6.4	L28M-R30Q		SVR
P-11	CT	6.8			D/C at Wk12 due to AE; SVR
P-12	CT	6.4	Q54H-P58S-Q62E		SVR
P-13	CT	7.4	Q54H		D/C at Wk6; PDR not achieved[c]
P-14	CT	6.5			SVR
P-15	CT	6.3	R30Q/R-Q62Q/R		SVR
P-16	CT	6.6	Q54H		SVR
P-17	CT	6.6	Q54H-Q62E		SVR
P-18	CT	6.9	Q54Y	Q80L	SVR
P-19	CT	6.6	Q54H-Y93H	N77A	SVR
P-20	CT	7.0	R30Q	S122G	SVR
P-21	CC	6.6	Q54L		SVR

[a]All NS3 and NS5A amino acids were examined with focus on polymorphisms at positions known to be associated with resistance to NS3 protease inhibitors (36, 43, 54, 55, 77, 78, 79, 80, 122, 123, 138, 155, 156, 158, 168, 170, 175) and NS5A inhibitors (21, 23, 24, 28, 30, 31, 32, 54, 58, 62, 92, 93). When a mixture of substitutions is indicated, the most predominant is identified first.
[b]HCV RNA undetectable at post-treatment week 24.
[c]PegIFN-α/RBV added; HCV RNA undetectable at post-treatment week 24 following 52 weeks of therapy.
AE, adverse event; D/C, discontinued; GT, genotype; HCV, hepatitis C virus; PDR, protocol-defined response; SAE, serious adverse event; SVR, sustained virologic response; Wk, week.

with NS3-S122G (P-20, no fold-change to either DCV/ASV), or NS5A-Q54H (P-13, no fold-change to DCV). P-13 was the only patient with HCV RNA <15 IU/ml (target detectable) at week 6 and was, therefore, considered a treatment failure. Treatment-emergent resistance at week 1 in the five patients could not be determined because of PCR failure. A comparison of initial virologic response vs. dose and polymorphisms associated with resistance revealed no differences. Among null responders who received ASV 600 mg, mean HCV RNA declines at week 1 for those with vs. without RAVs were −4.6 vs. −4.3 $\log_{10}$ IU/ml, which were similar to the week 1 declines among those who received ASV 200 mg (−4.5 $\log_{10}$ IU/ml with RAVs [one patient] vs. −4.3 $\log_{10}$).

Baseline HCV RNA levels did not have an impact on response to treatment; patients with high baseline viral load still experienced rapid and robust responses to therapy (Fig. 1; Table 1).

Ineligible/intolerant patients
Virologic response.
Virologic response at week 4 was greater in PegIFN-α/RBV ineligible patients than in null responders. Undetectable HCV RNA at week 4 was observed in 86% of the ineligible group vs. 52% of null responders. However, by week 12, undetectable HCV RNA was similar in both groups. Early HCV RNA declines appeared unaffected by *IL28B* genotype, the presence of baseline polymorphisms associated with resistance, or virologic outcome (Fig. 3). Adherence to therapy, assessed through pill counts, was

found to be high in six of the seven patients experiencing virologic failure. However, DCV/ASV exposures were high in the one non-compliant patient (P-31) who subsequently experienced relapse.

Baseline analysis.
Baseline *IL28B* genotype, polymorphisms associated with resistance, and virologic outcome are shown in Table 2 and Fig. 2B. Three patients presented with DCV resistance at baseline: one (P-25) with an NS5A-L31M-Y93H combination (7105-fold DCV resistance [13]) and two with an NS5A-Q54Y-Y93H (58-fold resistance). All three subsequently experienced viral breakthrough at week 10 or 16.

Other patients had baseline polymorphisms conferring minimal or low-level resistance to DCV and/or protease inhibitors; NS5A-Y93H (n = 4), NS5A-L28M-R30L (n = 1), NS3-T54S (n = 1), and NS3-Q80L (n = 5). Variable responses were observed among these patients (Fig. 2B); the majority responded, but two patients with baseline NS5A-Y93H experienced post-treatment relapse. One patient (P-24) with baseline NS5A-L28M-R30L-Q54H-A92T and NS3-Q80L-S122G had a slower response to treatment at week 1 when compared with mean HCV RNA reductions (SD) for ineligible/intolerant patients on the study (−3.4 vs. −4.74 [0.58] $\log_{10}$ IU/ml), but subsequently achieved SVR with only 16 weeks of treatment. Neither NS3-Q80L-S122G nor NS5A-L28M-R30L-Q54H-A92T conferred resistance to ASV or DCV, respectively.

Baseline viral load did not appear to affect response; mean HCV RNA levels (SD) were 6.4 (0.7) $\log_{10}$ IU/ml among patients

Table 2. Baseline viral and host characteristics among genotype-1b ineligible/intolerant patients and their virologic outcome.

Patient	IL28B GT	HCV RNA, log$_{10}$ IU/ml	NS5A polymorphism(s)[a]	NS3 polymorphism(s)[a]	Virologic outcome
P-22	CC	7.1			SVR
P-23	CC	6.9	A92T	Q80L-S122G/S	SVR
P-24	CC	6.6	L28M-R30L-Q54H-A92T	Q80L-S122S/G	D/C at Wk12 due to AE; SVR
P-25	CT	6.8	L31M/L-Y93H/Y		VBT (Wk16)
P-26	CC	5.3			SVR
P-27	CC	6.9	Q54H-Y93H/Y	T54S	SVR
P-28	CC	6.8	Y93H/Y	Q80L	SVR
P-29	CT	6.7	Q54Y-Y93H/Y	Q80L	VBT (Wk16)
P-30	CT	6.7	Q54H		SVR
P-31	CC	6.6	P58S/P-Y93Y/H	S122G	Relapse (FU Wk12)
P-32	CT	6.7	P58L	S122G	Relapse (FU Wk4)
P-33	CT	5.2	Q54H-Q62P/S		D/C at Wk12 due to patient request; SVR
P-34	CC	6.6		Q80L	SVR
P-35	CC	6.4	Q54H-Q62E/A-A92T		SVR
P-36	CC	7.1		S122S/C	Relapse (FU Wk4)
P-37	CC	6.6	Y93H		Relapse (FU Wk4)
P-38	CC	7.5		S122T	SVR
P-39	CC	5.1	R30Q/R		SVR
P-40	CC	6.8	Q54H-A92A/T	Q80L	D/C at Wk8[b]
P-41	CC	6.0		S122G	SVR
P-42	CC	6.5	A92T		SVR
P-43	CT	7.0	Q54Y-Y93H	S122G	VBT (Wk10)

[a]All NS3 and NS5A amino acids were examined with focus on polymorphisms at positions known to be associated with resistance to NS3 protease inhibitors (36, 43, 54, 55, 77, 78, 79, 80, 122, 123, 138, 155, 156, 158, 168, 170, 175) and NS5A inhibitors (21, 23, 24, 28, 30, 31, 32, 54, 58, 62, 92, 93). When a mixture of substitutions is indicated, the most predominant is identified first.
[b]Treatment discontinued at patient request; subsequently lost to follow-up.
AE, adverse event; D/C, discontinued; FU, follow-up; GT, genotype; HCV, hepatitis C virus; SVR, sustained virologic response; VBT, viral breakthrough; Wk, week.

achieving SVR compared with 6.8 (0.3) log$_{10}$ IU/ml among patients experiencing virologic failure. However, four of six patients with the IL28B CT allele subsequently failed treatment (three breakthroughs, one relapse) vs. only three of 16 patients with IL28B CC (all relapsed).

Genotypic analysis of patients with viral breakthrough.
Treatment-emergent RAVs were assessed through post-treatment week 48 in the three patients with virologic breakthrough (Table 3).

Patient P-25: This patient had an IL28B CT genotype with a baseline HCV RNA level of 6.8 log$_{10}$ IU/ml and a linked baseline NS5A-L31M-Y93H/Y polymorphism. Despite undetectable HCV RNA by week 4 (Fig. 4A), viral breakthrough occurred at week 16, associated with high-level resistance to both DCV (NS5A-L31M-P58A-Y93H; 65,000-fold) and ASV (D168A; ~120-fold in GT1b). Other minor variants detected at baseline by clonal analysis (NS5A-Q62R, -A92T) were not present at breakthrough. NS5A variants present at the end of therapy persisted through follow-up week 48, and, although P58A had largely changed to P58G (73% of 33 clones, Fig. 5A) by week 36, a similar ratio of P58G to A was detected at follow-up week 48. By contrast, NS3-D168A had mostly been replaced by wild type at week 48 (83% of 64 clones).

Patient P-29: This patient had an IL28B CT genotype, with a baseline HCV RNA level of 6.7 log$_{10}$ IU/ml and a pre-existing linked NS5A-Q54Y-Y93H/Y and NS3-Q80L (Fig. 5B). Undetectable HCV RNA by week 3 was followed by viral breakthrough at week

16 (Fig. 4A) associated with NS5A-L31M-Q54Y-Y93H (6467-fold DCV resistance) and NS3-Q80L-D168V (~280-fold ASV resistance). These RAVs remained stable through 48 weeks post-treatment.

Patient P-43: This patient had an IL28B CT genotype with a baseline HCV RNA level of 7.0 log$_{10}$ IU/ml, and a pre-existing NS5A-Q54Y-Y93H variant (Fig. 5C). HCV RNA was undetectable at week 2, and breakthrough occurred at week 10 (Fig. 4A), which was associated with a linked NS5A-L31M-Q54Y-Y93H variant (Fig. 5C; 6467-fold DCV resistance) and an NS3-D168V variant (~270-fold ASV resistance). Again, NS5A variants remained stable through week 48 post-treatment, while NS3-D168V was replaced by wild type (100% of 60 clones).

For the three patients experiencing viral breakthrough, DCV and ASV trough exposures were less than drug levels required to achieve a 90% effective concentration (EC$_{90}$) value against emergent RAVs (Table 3).

Genotypic analysis of patients experiencing post-treatment relapse.
Four ineligible patients, with undetectable HCV RNA at the end of treatment, experienced relapse (Fig. 4B). Resistance polymorphisms through week 48 off-treatment are shown in Table 3. Baseline polymorphisms associated with resistance were not detected in two patients (P-32 and P-36), but both displayed post-relapse resistance by follow-up weeks 8 and 4, respectively. Patient P-32 relapsed with NS5A-L31M-P58L-Y93H (8300-fold DCV resistance) and NS3-D168V (270-fold ASV resistance).
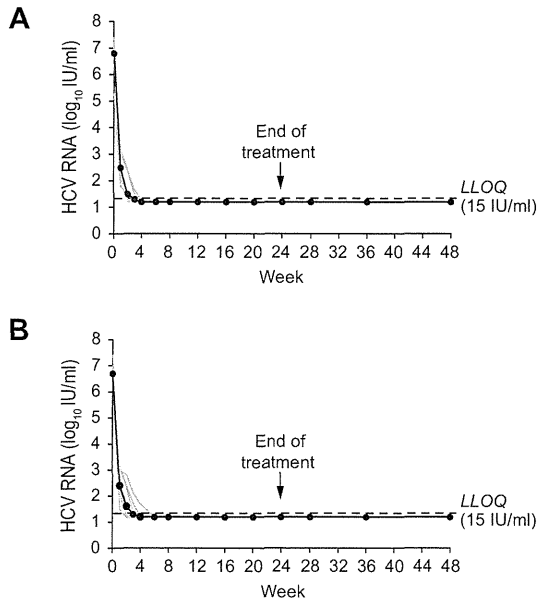
A

B

Fig. 1. HCV RNA levels among genotype-1b null responders. Treatment was initiated with (A) asunaprevir 600 mg BID or (B) asunaprevir 200 mg BID, in combination with daclatasvir 60 mg QD. Individual patient HCV RNA levels are shown in grey. Mean HCV RNA levels are shown in black. BID, twice daily; HCV, hepatitis C virus; LLOQ, lower limit of quantitation; QD, once daily.
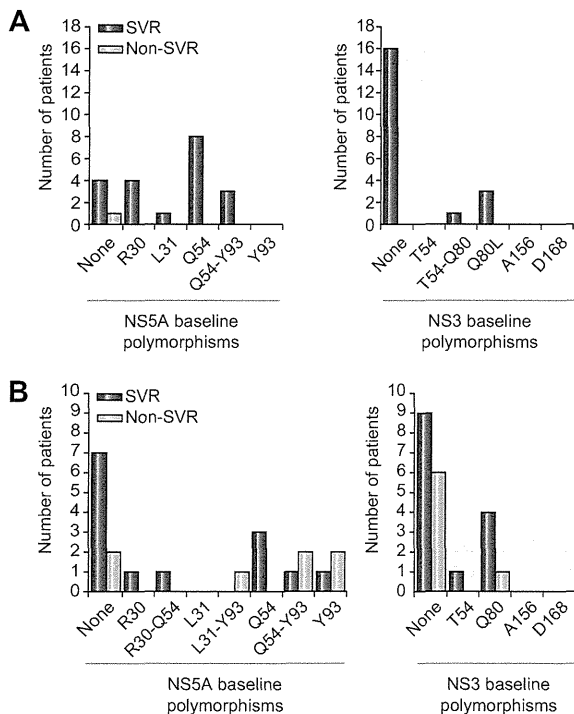
A

B

Fig. 2. Impact of baseline polymorphisms associated with resistance on virologic outcome among genotype-1b (A) null responders or (B) ineligible/intolerant patients. The ineligible/intolerant analysis excludes one patient (P-40) who discontinued therapy and was subsequently lost to follow-up. SVR, sustained virologic response.
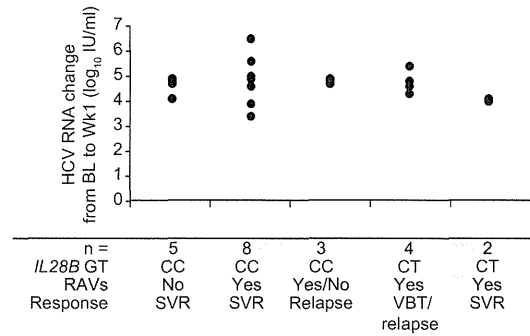

n =	5	8	3	4	2
IL28B GT	CC	CC	CC	CT	CT
RAVs	No	Yes	Yes/No	Yes	Yes
Response	SVR	SVR	Relapse	VBT/ relapse	SVR

Fig. 3. Early (week 1) declines in HCV RNA were similar among PegIFN-α/RBV ineligible or intolerant patients with and without baseline polymorphisms associated with resistance, virologic failure, and IL28B CT genotype. BL, baseline; GT, genotype; HCV, hepatitis C virus; RAV, resistance-associated variant; SVR, sustained virologic response; VBT, viral breakthrough.

Patient P-36 relapsed with an NS5A-L31V/M-Y93H genotype (L31V-Y93H: 14,789-fold DCV resistance vs. L31M-Y93H: 7105-fold) [13] and NS3-D168V. The remaining two patients had detectable NS5A-Y93H at baseline (24-fold DCV resistance) and additional substitutions at NS5A-L31 and NS3-D168 were detected after relapse. Patient P-31 displayed NS5A-L31M-Y93H (7105-fold DCV resistance) [13] and NS3-D168A (~120-fold ASV resistance); patient P-37 relapsed with the same NS5A-L31V/M-Y93H and NS3-D168V, as described for patient P-36.

Baseline HCV RNA and IL28B genotype did not appear to influence relapse; three of four relapse patients were IL28B CC genotype, and baseline HCV RNA was not appreciably higher than for those with SVR (mean HCV RNA [SD]: 6.8 [0.4] vs. 6.4 [0.7] $\log_{10}$ IU/ml, respectively).

Changes in the DCV resistance pattern present at relapse through follow-up week 48 were seen in three of four relapsers, with Y93H changing to wild type (100% of 68 clones) in patient P-32. Clonal analysis of the baseline sequence revealed the presence of Y93H as a minor species (~2%; 1/61 clones). Genotypic changes resulting in a lower level of phenotypic resistance (L31V-Y93H to L31M-Y93H) were detected in patients P-36 and P-37. NS3 substitutions observed at relapse were not detectable by population sequencing by follow-up week 36. The D168V substitution detected in patient P-37 was replaced by D168E (78-fold ASV resistance [19]) at follow-up weeks 36 and 48. As with the patients who experienced virologic breakthrough, ASV and DCV trough values in the three drug-compliant patients who relapsed were less than the observed EC_{90} values for the respective RAVs.

Discussion

This study assessed resistance and virologic failure in a difficult-to-treat population of null responders and PegIFN-α/RBV ineligible/intolerant patients treated with the dual oral combination of DCV and ASV. Overall, 77% achieved an SVR [11], with all viral breakthroughs and post-treatment relapses occurring in the ineligible/intolerant subpopulation. It is possible that pharmacokinetics may have played a role in these failures, since patients experiencing failure had DCV and/or ASV trough values below median or documented non-compliance [11]. However, since

Table 3. Emergence of resistance-associated variants among genotype-1b ineligible/intolerant patients experiencing viral breakthrough or relapse.

Patient	Time point	DCV/ASV C_{trough} range, nM	NS5A RAVs				DCV EC_{90}, nM	NS3 RAVs			ASV EC_{90}, nM
			L31	Q54	P58	Y93		Q80	S122	D168	
VBT patients											
P-25	BL		M/L	-	-	H/Y	<137	-	-	-	
	Wk16 (VBT)		M	-	A	H	>1000	-	-	A	540
	Wk20		V	-	A	H		-	-	A	
	Wk24	190-261/25-41	M	-	A	H		-	-	A	
	FU Wk4		M	-	A	H		-	-	A	
	FU Wk36		M	-	G	H	>5000	-	-	D/A	
	FU Wk48		M	-	G/A	H		-	-	-	
P-29	BL		-	Y	-	H	0.04	L	-	-	1.6
	Wk16 (VBT)		ND	ND	ND	ND	ND	ND	ND	ND	ND
	Wk20	116-198/18-33	M/V	Y	-	H	750	L	-	V	55
	FU Wk4		M	Y	-	H		L	-	V	
	FU Wk36		M	Y	-	H		L	-	V	
	FU Wk48		M	Y	-	H		L	-	V	
P-43	BL		-	Y	-	H	0.49	-	G	-	2.8
	Wk10 (VBT)		M	Y	-	H	435	-	G	V	279
	FU Wk4	243/69	M	Y	-	H		-	G	V	
	FU Wk36		M	Y	-	H		-	G	-	
	FU Wk48		M	Y	-	H		-	G	-	
Relapse patients											
P-31	BL	573-620/	-	-	S/P	Y/H	0.02	-	G	-	
	FU Wk16	153-327	ND					-	-	A	
	FU Wk24		M	-	-	H	351	-	G	-	
	FU Wk36		-	-	-	-		-	-	-	
	FU Wk48		-	-	-	-		-	-	-	
P-32	BL	151-306/19-42	-	-	L	-	0.004	-	G	-	
	FU Wk8		M	-	L	H		-	G	V/D	
	FU Wk12		M	-	L	H	543	-	G	-	
	FU Wk36		M	-	L	-	1.5	-	G	-	
	FU Wk48		M	-	L	-		-	G	-	
P-36	BL	138/26	-	-	-	-		-	-	-	
	FU Wk8		V/M	-	-	H		-	-	V	1190
	FU Wk12		V	-	-	H	349	-	-	-	
	FU Wk24		M/V	-	-	H		-	-	V/D	
	FU Wk36		M	-	-	H	137	-	-	-	
	FU Wk48		M	-	-	H		-	-	-	
P-37	BL	75-134/40-93	-	-	-	H	0.49	-	-	-	
	FU Wk8		V	-	-	H		-	-	V	
	FU Wk12		V/I	-	-	H		-	-	V	
	FU Wk24		M	-	-	H		-	-	V	
	FU Wk36		M	-	-	H		-	-	E/D	
	FU Wk48		M	-	-	H		-	-	-	

When a mixture of substitutions is indicated, the most predominant is written first. ASV-resistant variants conferred no cross-resistance to DCV and *vice versa* in a replicon assay. Dashes indicate consensus with control sequence GT1b (Con1).

ASV, asunaprevir; BL, baseline; DCV, daclatasvir; EC_{90}, 90% effective concentration; FU, follow-up; ND, not determined as multiple amplifications failed; RAV, resistance-associated variant; VBT, viral breakthrough; Wk, week.

most patients with troughs below the median achieved SVR, the influence of drug exposure is hard to assess.

NS5A-Y93H was identified as the predominant polymorphism at baseline in all three patients with viral breakthrough and in two of the four patients with relapse. However, three null responders and two ineligible/intolerant patients also had a pre-existing NS5A-Y93H polymorphism and all achieved SVR, making the significance of Y93H alone, for response in the broader patient population, difficult to assess. Furthermore, where Y93H polymorphisms existed at baseline, their effects on
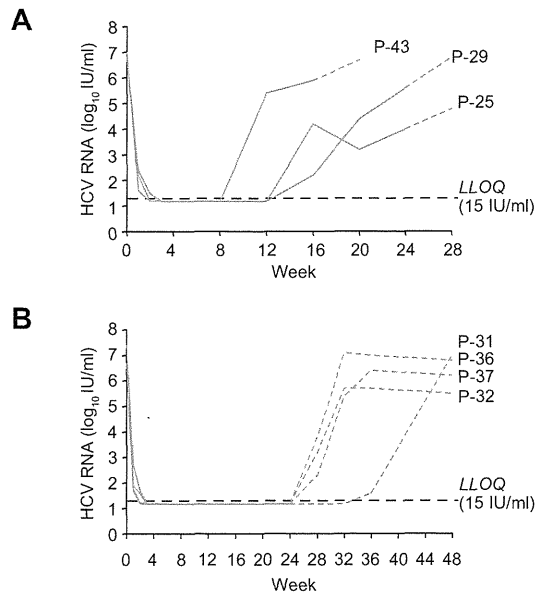
Research Article

Fig. 4. HCV RNA levels on-treatment and during post-treatment follow-up for genotype-1b ineligible/intolerant patients experiencing (A) viral breakthrough or (B) relapse. Solid lines indicate on-treatment period. Dashed lines indicate post-treatment follow-up. HCV, hepatitis C virus; LLOQ, lower limit of quantitation.

Fig. 5. Clonal analysis of NS3 protease and NS5A resistance-associated variants in patients experiencing virologic breakthrough. (A) Patient P-25. NS5A RAV: baseline 30 clones; Wk16 39 clones; FU Wk36 33 clones; FU Wk48 not performed (no change from FU Wk36 by population sequencing). NS3 RAV: baseline 32 clones; Wk16 41 clones; FU Wk36 56 clones; FU Wk48 63 clones. (B) Patient P-29. NS5A RAV: baseline 37 clones; Wk20 50 clones; FU Wk36/48 analyses not performed (no change from VBT by population sequencing). NS3 RAV: baseline 34 clones; Wk20 47 clones; FU Wk36/48 analyses not performed (no change from VBT by population sequencing). (C) Patient P-43. NS5A RAV: baseline 32 clones; Wk10 47 clones; FU Wk36/48 analyses not performed (no change from VBT by population sequencing). NS3 RAV: baseline 31 clones; Wk10 32 clones; FU Wk36 103 clones; FU Wk48 60 clones. FU, follow-up; VBT, viral breakthrough; RAV, resistance-associated variant.

DCV inhibition were minimal (Y93H EC_{50} = 49 pM [6]) compared with C_{trough} values that ranged from 75 to 620 nM. The global prevalence of NS5A-Y93H is approximately 4%, based on data from the Los Alamos database [20] and unpublished data from nine DCV studies, and is approximately 11% in other recent Japanese DCV studies [21], which is considerably lower than the 23% (10/43) prevalence observed in this study. Further analysis of DCV study data indicates that Y93H pre-exists at higher levels in patients infected with GT1b (10%) than GT1a (1%); however, the link with *IL28B* is not so clear given that most failures to date with DCV have been observed in GT1a patients with no baseline Y93H. Other polymorphisms observed at a higher frequency among this GT1b population included NS3-Q80L (~19%, 8/43) vs. Q80K, which has been observed more frequently in GT1a populations [18,19].

Baseline HCV RNA did not appear to influence virologic response in either population, and response was too rapid to allow successful genomic sequencing after 1 week of treatment. ASV dose (600 mg or 200 mg twice daily) did not impact the initial decline in HCV RNA in null responders, and the *IL28B* CT allele, present in 86% (18/21) of null responders, did not prevent patients from achieving a very high (90%) SVR. By contrast, although only 27% (6/22) of ineligible/intolerant patients were *IL28B* CT, this genotype was present in all three viral breakthroughs and one of four relapses. While *IL28B* genotype is known to influence response to PegIFN-α/RBV, its apparent impact on virologic suppression in alfa-sparing regimens is unexpected. However, given the small number of patients, any such correlation will require evaluation in a larger dataset.

The emergent RAVs at viral breakthrough or relapse (signature NS5A-L31 and -Y93 substitutions for DCV and NS3-D168 substitutions for ASV) were similar to observations from other
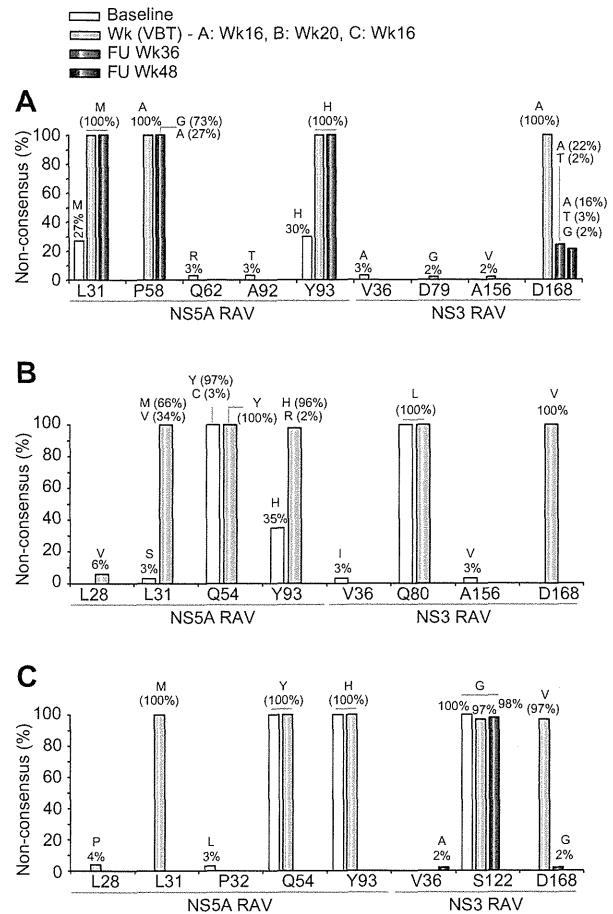
clinical studies of DCV, and from *in vitro* GT1b replicon resistance studies with ASV [19], although this study represents the first demonstration of emergent clinical ASV resistance. It is possible that signature resistance variants to both DCV and ASV pre-existed as minor species, and subsequently enriched by selective pressure, as predicted by viral kinetic modeling [22]. Although a combination of these NS3 and NS5A variants was not detected by clonal sequencing at baseline, their low-level pre-existence cannot be ruled out. However, assessment of minor NS3 plus NS5A variants from the same RNA sequence is currently not feasible using available deep-sequencing technologies. Nevertheless, additional studies to assess the presence and dynamics of minority baseline variants under drug selection are indicated.

Interestingly, ASV-resistant NS3-D168 substitutions generally decayed during the off-drug follow-up period, implying a lack of replicative fitness relative to wild type, in the absence of selective drug pressure. Indeed, a reduction in replicative fitness has been observed for D168 variants in replicons [19]. Neither of the secondary variants associated with D168V in this study (Q80L or S122G) had an impact on fitness in vitro (replication capacity similar or higher than that observed for parental GT1b [Con1] replicon), with both double variants possessing replicative capacities similar to D168V alone [19]. However, clonal analysis indicated that ASV-resistant variants were still detectable in some post-treatment samples as minority species, although not detectable by population sequencing. Deeper sequencing techniques will be required to fully establish the dynamics of decay and whether ASV-resistant strains remain enriched for long periods relative to baseline. Since the re-treatment of patients with prior NS3 protease inhibitor failure has only been assessed in small studies [23], it is not clear whether these NS3 RAVs will form a stable minority capable of rapid overgrowth on re-treatment. By contrast, NS5A variants associated with DCV resistance were observed to be linked and relatively stable through at least 48 weeks post-treatment, although change of DCV-resistance substitutions was noted in four of seven patient samples. As described above, the prevalence of the NS5A variant Y93H, which confers low level resistance to DCV, is approximately 10% in the general HCV GT1b population. Linked NS5A RAVs conferring high level resistance to DCV are less prevalent (<1%). While NS3 RAVs (substitutions at positions V36, T54, R155, or D168) associated with first-generation protease inhibitors have been reported to be present at ≤2.7% by population sequencing [5,24], emergent NS3 RAVs have been shown to persist for up to 4 years in long-term follow-up studies [25]. Therefore, longer-term studies are indicated to assess what, if any, replicative impairment is conferred by these linked NS5A changes and how long these potentially transmissible drug-resistant strains persist without DCV selection pressure.

In conclusion, high response rates were achieved in this small Japanese study comprising GT1b null responders and PegIFN-α/RBV ineligible/intolerant patients with limited treatment options. Among patients experiencing virologic failure, ASV- and DCV-resistant substitutions emerged together at the time of failure, which were similar to those reported previously. An analysis of persistence demonstrated that DCV-resistant substitutions appeared to have greater fitness over the duration of the study. A loose association with a baseline NS5A polymorphism on virologic outcome was observed; however, further data from larger studies are required. Consequently, a greater understanding of the role and dynamics of pre-existing, emergent, and persistent resistance variants to DCV and ASV will be sought from the planned phase 3 global studies of this combination.

Financial support

Conflict of interest

References

[1] Jacobson IM, McHutchison JG, Dusheiko G, Di Bisceglie AM, Reddy KR, Bzowej NH, et al. Telaprevir for previously untreated chronic HCV infection. N Engl J Med 2011;364:2405-2416.

[2] Poordad F, McCone J, Bacon BR, Bruno S, Manns MP, Sulkowski MS, et al. Boceprevir for untreated chronic HCV genotype 1 infection. N Engl J Med 2011;364:1195-1206.

[3] Ghany M, Nelson DR, Strader DB, Thomas DL, Seeff LB. An update on treatment of genotype 1 chronic HCV infection: 2011 practice guidelines by the American Association for the Study of Liver Diseases. Hepatology 2011;54:1433-1444.

[4] Merck. VICTRELIS™ (boceprevir) [package insert]; 2012.

[5] Vertex Pharmaceuticals. INCIVEK™ (telaprevir) [package insert]; 2012.

[6] Gao M, Nettles RE, Belema M, Snyder LB, Nguyen VN, Fridell RA, et al. Chemical genetics strategy identifies an HCV NS5A inhibitor with a potent clinical effect. Nature 2010;465:96-100.

[7] Pol S, Ghalib RH, Rustgi VK, Martorell C, Everson GT, Tatum HA, et al. Daclatasvir for previously untreated chronic hepatitis C genotype-1 infection: a randomised, parallel-group, double-blind, placebo-controlled, dose-finding, phase 2a trial. Lancet Infect Dis 2012;12 (9):671-677.

[8] McPhee F, Sheaffer AK, Friborg J, Hernandez D, Falk P, Zhai G, et al. Preclinical profile and characterization of the hepatitis C virus NS3 protease inhibitor asunaprevir (BMS-650032). Antimicrob Agents Chemother 2012;56: 5387-5396.

[9] Bronowicki JP, Pol S, Thuluvath P, Larrey D, Martorell CT, Rustgi VK, et al. Asunaprevir (ASV; BMS-650032), an NS3 protease inhibitor, in combination with peginterferon and ribavirin in treatment-naive patients with genotype 1 chronic HCV infection. J Hepatol 2012;56 (suppl 2):S431-S432.

[10] Chayama K, Takahashi S, Toyota J, Karino Y, Ikeda K, Ishikawa H, et al. Dual therapy with the NS5A inhibitor, daclatasvir, and the NS3 protease inhibitor, asunaprevir, in HCV genotype 1b-infected null responders. Hepatology 2012;55:742-748.

[11] Suzuki Y, Ikeda K, Suzuki F, Toyota J, Karino Y, Chayama K, et al. Dual oral therapy with daclatasvir and asunaprevir for patients with HCV genotype 1b infection and limited treatment options. J Hepatol 2013;58:655-662.

[12] Bronowicki JP, Pol S, Thuluvath PJ, Larrey D, Martorell CT, Rustgi VK, et al. BMS-650032, an NS3 inhibitor, in combination with peginterferon alfa-2a and ribavirin in treatment-naive subjects with genotype 1 chronic HCV infection. J Hepatol 2011;54 (suppl 1):S472.

[13] Fridell RA, Wang C, Sun JH, O'Boyle DR, Nower P, Valera L, et al. Genotypic and phenotypic analysis of variants resistant to HCV NS5A replication complex inhibitor BMS-790052: in vitro and in vivo correlations. Hepatology 2011;54:1924-1935.

[14] Pasquinelli C, McPhee F, Eley T, Villegas C, Sandy K, Wendelburg P, et al. Single and multiple ascending dose studies of the NS3 protease inhibitor asunaprevir in subjects with or without chronic hepatitis C. Antimicrob Agents Chemother 2012;56:1838-1844.

[15] Sheaffer AK, Lee MS, Hernandez D, Chaniewski S, Yu F, Falk P, et al. Development of a chimeric replicon system for phenotypic analysis of NS3 protease sequences from HCV clinical isolates. Antivir Ther 2011; 16:705-718.

Research Article

[16] Fridell RA, Qiu D, Wang C, Valera L, Gao M. Resistance analysis of the HCV NS5A inhibitor BMS-790052 in an in vitro replicon system. Antimicrob Agents Chemother 2010;54:3641–3650.

[17] Sun JH, O'Boyle DR, Zhang Y, Wang C, Nower P, Valera L, et al. Impact of a baseline polymorphism on the emergence of resistance to the HCV NS5A replication complex inhibitor BMS-790052. Hepatology 2012;55:1692–1699.

[18] Lenz O, Verbinnen T, Lin TI, Vijgen L, Cummings MD, Lindberg J, et al. In vitro resistance profile of the HCV NS3/4A protease inhibitor TMC435. Antimicrob Agents Chemother 2010;54:1878–1887.

[19] McPhee F, Friborg J, Levine S, Chen C, Falk P, Yu F, et al. Resistance analysis of the HCV NS3 protease inhibitor asunaprevir. Antimicrob Agents Chemother 2012;56:3670–3681.

[20] Kuiken C, Yusim K, Boykin L, Richardson R. The Los Alamos hepatitis C sequence database. Bioinformatics 2005;21:379–384.

[21] McPhee F, Hernandez D, Yu F, Ueland J, Chayama K, Toyota J, et al. A description of virologic escape in HCV genotype 1-infected patients treated with daclatasvir (BMS-790052) in combination with ribavirin and peginterferon-alfa-2a or peginterferon-alfa-2b. J Hepatol 2012;56 (suppl 2): S473.

[22] Guedj J, Rong L, Dahari H, Perelson AS. A perspective on modelling hepatitis C virus infection. J Viral Hepat 2010;17:825–833.

[23] Lenz O, de Bruijne J, Vijgen L, Verbinnen T, Weegink C, Van Marck H, et al. Efficacy of re-treatment with TMC-435 as combination therapy in HCV-infected patients following TMC-435 monotherapy. Gastroenterology 2012;143:1176–1178, e6.

[24] Kieffer TL, De Meyer S, Bartels DJ, Sullivan JC, Zhang EZ, Tigges A, et al. Hepatitis C viral evolution in genotype 1 treatment-naive and treatment-experienced patients receiving telaprevir-based therapy in clinical trials. PLoS One 2012;7:e34372.

[25] Susser S, Vermehren J, Forestier N, Welker MW, Grigorian N, Füller C, et al. Analysis of long-term persistence of resistance mutations within the hepatitis C virus NS3 protease after treatment with telaprevir or boceprevir. J Clin Virol 2011;52:321–327.

Original Article

Randomized controlled trial of a new procedure of radiofrequency ablation using an expandable needle for hepatocellular carcinoma

Miharu Hirakawa,[1] Kenji Ikeda,[2] Masahiro Kobayashi,[2] Yusuke Kawamura,[2]
Tetsuya Hosaka,[2] Hitomi Sezaki,[2] Norio Akuta,[2] Fumitaka Suzuki,[2] Yoshiyuki Suzuki,[2]
Satoshi Saitoh,[2] Yasuji Arase[1,2] and Hiromitsu Kumada[2]

[1]Health Management Center, and [2]Department of Hepatology, Toranomon Hospital, Tokyo, Japan

Aim: To evaluate the efficacy of a new ablation procedure for the stepwise hook extension technique using a SuperSlim needle for radiofrequency ablation (RFA) treatment of hepatocellular carcinoma (HCC), a randomized controlled trial was performed.

Methods: Thirty patients with HCC measuring 20 mm or less were randomly treated with a conventional four stepwise expansion technique (group 1) and the new stepwise expansion technique (group 2; the electrode was closed in the shaft after the same three steps of the conventional procedure and then fully extended). All patients underwent the RFA procedure using a 10-hook expandable electrode of 17-G diameter (LeVeen SuperSlim 30 mm). We compared the ablation time, required energy and ablated lesions in the two groups.

Results: The long and short diameters of RFA-induced necrosis were significantly larger in group 2 (37 and 28 mm) than group 1 (30 and 26 mm, $P = 0.001$ and $=0.045$, respectively). Irregular and small needle expansion resulting in the parachute-like or irregularly shaped ablated zone was observed in more cases in group 1 than in group 2. The new technique made all tines expand uniformly and largely, which produced a near-oval ablated zone of which the long axis is perpendicular to the needle shaft.

Conclusion: The two kinds of stepwise procedures allow the selection of a more suitable procedure according to the tumor size and shape in each RFA.

Key words: expandable needle, hepatocellular carcinoma, radiofrequency ablation, randomized controlled trial

INTRODUCTION

PERCUTANEOUS TREATMENT INCLUDING radiofrequency ablation (RFA) and percutaneous ethanol injection (PEI) is often used for small-size hepatocellular carcinoma (HCC) because it is less invasive than surgical therapy. RFA has become the first-choice local treatment because of the excellent outcome; the efficacy of RFA in HCC tumors measuring less than 2 cm in diameter is similar to that of PEI but it requires fewer treatment sessions, and the efficacy in HCC tumors of more than 2 cm in diameter is better than with PEI.[1] In addition, RFA is also more cost-effective than surgical

resection of small HCC.[2] With three commercially-available RFA apparatuses – the radiofrequency tumor coagulation system (RTC system; Boston-Scientific, Natick, MA, USA), radiofrequency interstitial thermal ablation system (RITA; AngioDynamics, Latham, NY, USA) and cool-tip RF system (Valleylab, a division of Tyco Healthcare Group, Boulder, CO, USA) – the volume ablated during one RFA session is of a diameter less than 3.0–4.0 cm, except in ablation with the Starburst XL RFA device (RITA).[3] RFA therapy is currently restricted to tumors measuring less than 3 cm. In this regard, previous studies reported that the necrotic area could be enlarged by saline injection prior to RFA,[4,5] combination of RFA with PEI,[6,7] RFA with ethanol lipiodol injection,[8] RFA with transcatheter arterial embolization[9] and RFA with transient arterial obliteration.[10–12]

Among the above three RFA apparatuses, the RTC system and RITA have adopted the use of expandable needles. We reported previously the efficacy of the

stepwise hook extension technique for RFA therapy of HCC.[13] The technique allows rapid roll-off at lower power and lower energy and reduces any possible increase in intra-tissue pressure that may cause scattering of intrahepatic metastasis.[14–17]

A more slender expandable needle has been developed (17-G, SuperSlim; Boston Scientific, Natick, MA, USA) for easier and safer insertion into the liver. However, insertion of the slim needle into the liver tissue could result in deformation of the needle and hence possible reduction of the size of the ablated area. To overcome this shortfall, we designed a new technique involving full re-expansion after stepwise extension, to ensure full expansion of the needle. We have already reported the experimental study using healthy pig livers *in vivo* to show that this technique can produce a larger necrotic zone than the conventional stepwise procedure.[18]

The aim of this study was to evaluate the efficacy of the new ablation procedure for the stepwise hook extension technique for RFA therapy of HCC of a patient with cirrhosis or without cirrhosis in a randomized controlled trial.

METHODS

Patients and tumors

FROM NOVEMBER 2006 to March 2010, 30 consecutive patients who met the following criteria were enrolled in this study: (i) HCC confirmed either histopathologically or radiologically; and (ii) diameter of the hepatic tumor of no more than 20 mm. They included 20 men and 10 women, with a median age of 57 years (range, 43–73). Seventeen patients were with cirrhosis and the other 13 were without cirrhosis. Table 1 lists the clinical background of patients of both groups. There were no significant differences between the groups.

A typical hypervascular HCC was diagnosed by typical hypervascular stain on digital subtraction angiography. In addition, one of the following three criteria was used to diagnose a tumor as a well-differentiated HCC: (i) histopathological diagnosis as well-differentiated HCC; (ii) hypo-enhanced lesion on computed tomography (CT) during hepatic arteriography (CTHA) and hypoperfusion on CT during arterial portography (CTAP); and (iii) hypo-enhanced lesion on the equilibrium phase of dynamic CT or hypo-perfused lesion on CTAP and hypointense on the hepatocyte-specific phase of multiple resonance imaging (MRI) using gadolinium-ethoxybenzyl-diethylenetriamine pentaacetic acid (Gd-EOB-DTPA) (Primovist; Bayer Schering Pharma, Osaka, Japan). A total of 30 patients were treated by the RFA protocol.

The study protocol was approved by the Human Ethics Review Committee of Toranomon Hospital and a signed consent form was obtained from each patient.

RFA protocol

We used the RTC system comprising a slim expandable needle (30 mm, 17-G LeVeen needle, SuperSlim), which consists of 10 expandable monopolar array electrodes, and the RF3000 generator, with a maximum power output of 120 W, and four electrode pads placed on the patient's skin. Instead of using the standard method recommended by the manufacturer, we adopted two types of stepwise hook extension techniques.[18] Patients were randomly divided into two groups based on the RFA protocol used. In group 1, after placing the needle electrode shaft into the tumor with the array retracted, using real-time ultrasound guidance, the electrode tines were expanded to a quarter, a half, three-quarters of the length and full-length in the first, second, third and final steps, respectively. The diameter of the array at each step was 10, 15, 25 and 30 mm, respectively. In group 2, the

Table 1 Background of the patients in groups 1 and 2

	Group 1 (conventional method)	Group 2 (new method)	P
Male : female	8:8	12:2	0.042
Age†	69 (45–82)	71 (60–84)	0.270
With cirrhosis : without cirrhosis	11:5	6:8	0.160
Tumor diameter, mm†	12 (9–18)	16 (6–19)	0.179
Hypervascular, yes : no	13:3	11:3	0.520

†Data are median (range).
NS, not significant.

first, second and third steps were similar to those of g1. After the third step, the tines were again closed within the shaft and then fully expanded.[18]

Power was first applied at 30 W and then increased at 10-W increments every minute in each step to a maximum of 120 W. The power was fixed once it reached 120 W. The necessary electric power and tissue impedance were recorded every 15 s. The procedure was applied continuously until a rise in impedance (caused by coagulation necrosis) with a corresponding drop in delivered power (a phenomenon called "roll-off"). The energy requirement for ablation was integration of the electric power (W) over the ablation time (s), which could be calculated approximately by summing a product of 15 (s) and the electric power measured every 15 s.

Image analysis

Tumor size, location and vascularity were evaluated before RFA using contrast-enhanced CT or MRI. Dynamic CT scans were performed using nonionic contrast material unless the patient was allergic to the iodine medium, for whom MRI was performed. Dynamic CT consisted of the arterial phase (30-s delay), hepatic portal phase (60-s delay) and hepatic venous phase (120-s delay) with slice thickness of 5 mm after the start of injection, respectively. Contrast-enhanced MRI was performed with i.v. injection of contrast material Gd-EOB-DTPA (EOB-MRI). Dynamic MRI consisted of the arterial phase (30-s delay), hepatic portal phase (60-s delay) and hepatic venous phase (120- and 180-s delay) with a thickness of 5 mm and hepatocyte-specific phase (>20 min delay) with a thickness of 3 mm. The tumor was appraised as "hypervascular" when it was stained denser on the arterial phase image compared to the surrounding liver parenchyma.

One to three days after the treatment, the size and shape of the RF-induced lesion was evaluated by measuring three perpendicular dimensions of portal phase images of the contrast-enhanced CT or MRI, calculating the hypothetical volume of the ablated zone. In cases in which CT/MRI images were taken along the needle trace and those perpendicular to the needle, we measured the length of the ablated area along the needle tract and the diameter of the area perpendicular to it.

Statistical analysis

The duration of ablation, required energy and the size of the ablated lesions were compared between the two groups using the Mann–Whitney U-test. All values were expressed as median. A P-value less than 0.05 denoted the presence of a statistically significant difference.

RESULTS

Ablation time and required energy

ROLL-OFF WAS achieved at each step of ablation in all 30 RFA procedures. Table 2 shows the time to reach roll-off at each step and total ablation time in the two groups. These results indicate that the durations of the first step, second step and third step were similar for groups 1 and 2 ($P = 0.356$, $= 0.457$ and $= 0.590$, respectively), while that of the fourth step and total session were longer for group 2 than group 1 ($P < 0.001$ and <0.001, respectively). The energy required for one procedure was 18.1 kJ (range, 10.7–31.3) and 59.9 kJ (range, 35.1–119.5) for groups 1 and 2, respectively, indicating more energy requirement for group 2 than group 1 ($P < 0.0001$).

Needle expansion

Figure 1 depicts CT images showing the tines in the tumor in the final step; Figure 1(a,b) shows a cross-

Table 2 Comparison of ablation time (in min/s) and radio frequency-induced areas between groups 1 and 2

|	Group 1	Group 2	P
Duration of the first step	1′ 53″ (0′ 54″–3′ 43″)	2′ 37″ (1′ 00″–4′ 34″)	0.356
Second step	2′ 14″ (0′ 40″–4′ 57″)	2′ 21″ (0′ 16″–3′ 35″)	0.457
Third step	1′ 26″ (0′ 52″–2′ 46″)	1′ 30″ (0′ 57″–4′ 38″)	0.590
Fourth step	1′ 36″ (1′ 02″–3′ 55″)	9′ 20″ (6′ 39″–17′ 13″)	<0.001
Total ablation time	7′ 36″ (5′ 07″–10′ 13″)	15′ 07″ (11′ 22″–25′ 05″)	<0.001
Required energy for ablation, kJ	18.1 (10.7–31.3)	59.9 (35.1–119.5)	<0.001
Long diameter, mm	30 (21–37)	37 (31–60)	0.001
Short diameter, mm	26 (16–32)	28 (25–39)	0.045
Axial diameter, mm	35 (20–45)	40 (30–50)	0.018

Data are median (range).
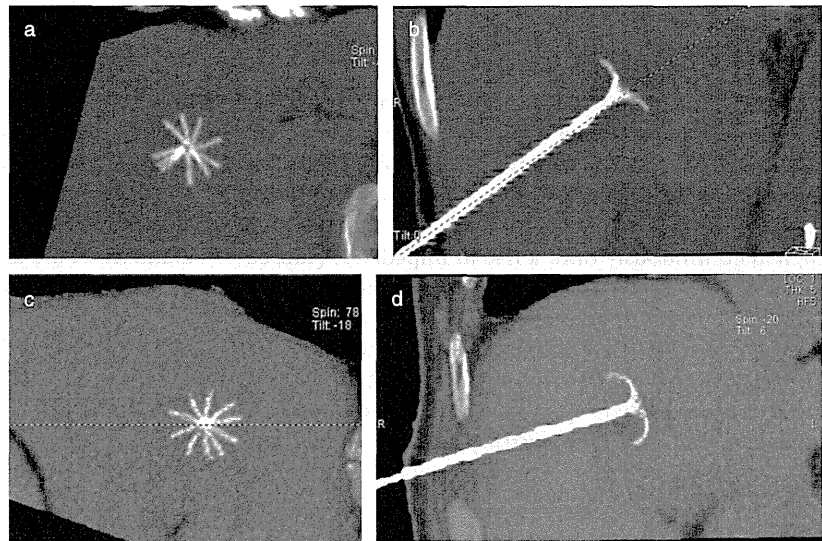
Figure 1 Electrode tines in the final step. (a,b) Tines are uniformly and fully expanded. (c,d) Tines are irregularly and insufficiently expand.

section perpendicular to the needle axis and that along the axis of group 1. Figure 1(c,d) shows those of group 2. All tines are almost uniformly extended as shown in Figure 1(c), while two tines remained attached to each other in Figure 1(a). We checked for needle expansion during RFA in six cases; three cases of group 1 and three cases of group 2. No uniform expansion was detected in any of the cases (0%) of group 1 and 2 cases (67%) of group 2, while irregular expansion was identified in three cases (100%) of group 1 and one case (33%) of group 2. Furthermore, the extent of the expansion at the final step was larger in Figure 1(b) than in (d).

Size and shape of ablated tissue

Table 2 also shows the long and short diameters of the axial cross-section and axial length of the ablated lesions measured on CT images in the two groups. The long diameter was 30 mm (range, 21–37) in group 1 and 37 mm (range, 31–60) in group 2. The short diameter was 26 mm (range, 16–32) in group 1 and 28 mm (range, 25–39) in group 2. The axial length was 35 mm (range, 20–45) in group 1 and 40 mm (range, 30–50) in group 2. All three diameters of group 2 were significantly longer than those of group 1.

In six patients, we reconstructed the post-RFA CT images to show the length of the ablated zone along the shaft and its vertical diameter (Fig. 2). When the tines were uniformly expanded as shown in Figure 1(c), the cross-sectional shape of the ablated zone perpendicular to the axis was nearly circular (Fig. 2c). The zone was more irregular when the tines were non-uniformly sepa-

rated (see Fig. 1a); the cross-section was also irregular in shape similar to Figure 1(a). In the former case, the ablated zone along the shaft was near-oval in shape with the short axis equivalent to the shaft (Fig. 2d), while the shape was parachute-like or was irregularly shaped sometimes in the latter case (Fig. 2b).

Comparison of the long and short diameters in patients with cirrhosis and without cirrhosis showed that neither the long axis nor the short axis were significantly different; the long diameters in patients with cirrhosis and without cirrhosis were 33 mm (range, 21–53) and 32 mm (range, 25–60), respectively ($P = 0.451$). The short diameter in patients with cirrhosis and without cirrhosis were 27 mm (range, 16–39) and 27 mm (range, 21–36), respectively ($P = 0.983$).

Complications

We did not encounter any episodes of heat injury to adjacent organs, skin burn, symptomatic pleural effusion, intrahepatic abscess, intraperitoneal bleeding or renal failure in either group.

DISCUSSION

RADIOFREQUENCY ABLATION THERAPY is one of the curative therapies for HCC measuring less than 30 mm in diameter, whereas surgical resection is the only curative treatment for HCC of more than 30 mm and less than 50 mm in diameter. However, surgical resection cannot be performed in patients with severe liver dysfunction or severe vascular invasion. In Japan,
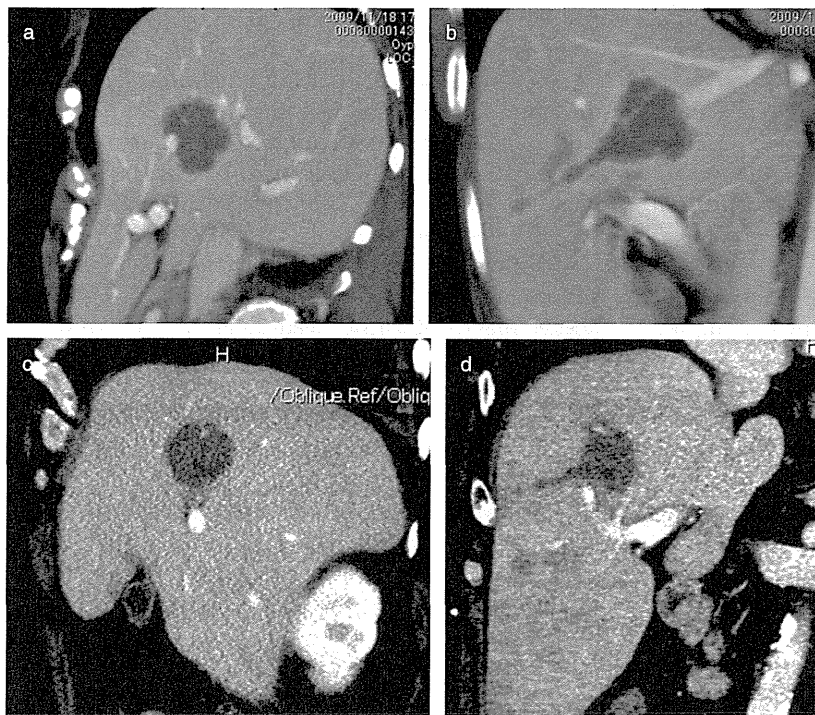
Figure 2 Dynamic computed tomography images of post-radiofrequency ablation lesions produced by the conventional procedure (group 1) and the new procedure (group 2). (a) The shape of the lesion perpendicular to the axis in group 1 is irregular. (b) The shape of the lesion along the axis in group 1 is parachute-like. (c) The shape perpendicular to the axis in group 2 is nearly circular. (d) The shape along the axis in group 2 is ellipsoid.

the Japan Society of Hepatology issued consensus-based HCC treatment guidelines in 2010, which include a HCC treatment algorithm. In this algorithm, resection can be selected with a patient with liver function Child–Pugh class A/B and without vascular invasion or with Vp1 or 2.[19] Thus, a technique that widens the RF-ablated area can improve, at least theoretically, the survival of cirrhotic patients with HCC over 30 mm in diameter.

The shape of the ablated zone depends on the needle type.[3] For example, the path along the shaft is longer than the transverse diameter when using the cool-tip electrode (cool-tip RF system), shorter when using the expandable needle of the RTC system and compatible with each other when using the LeVeen needle (RITA system). The shorter path is less disadvantageous than the shorter perpendicular diameter, because the ablated zone along with the needle trace can be enlarged by repeating the procedure as the needle is extracted while that perpendicular to the tract cannot be enlarged during one insertion. Although it is often difficult to achieve roll-off during a single-step full expansion procedure using the LeVeen needle, our stepwise procedure[13] overcomes this difficulty and produces an oval ablation zone similar to the single-step procedure. The more slender expandable LeVeen Superslim needle is

easier and safer to insert into the liver. However, it is easier to deform during insertion and hardly extend as expected; it cannot be fully extended when expanded slowly. This is because the shaft is pushed back as the electrode is inserted toward the liver. To overcome this inconvenience, we designed a new technique, full re-expansion after stepwise extension, which allows a sharper and definite expansion of the slim needle to full length.

We have demonstrated in our previous experimental study,[18] using the pig liver *in vivo*, that the new extension procedure for the expandable needle allows coagulation of a larger and more oval lesion even when using the slim needle. One of the differences between the pig experimental study and the clinical study is that RFA is applied in patients with HCC who have chronically damaged livers. The results showed that the new procedure can also produce a larger ablated zone of which the long axis is perpendicular to the needle shaft compared to that of the conventional procedure in chronically damaged livers; the size of the ablated zone was independent of the liver architecture and liver fibrosis.

The ablation times in this clinical study were similar to those of the experimental studies; the duration of the first, second and third steps were similar in groups 1 and

2, while those of the fourth step and total session were longer in group 2 than group 1. The energy required for one procedure was larger in group 2 than in group 1. The roll-off phenomenon represents marked increase in tissue impedance due to coagulation necrosis. In other words, once the roll-off occurs, the tissue in contact with tines is isolated. Thus, the additional electric current and energy cannot be introduced when the positions of tines are kept in the same position just after the roll-off. After the humors soaks into necrotic tissue from outside normal liver tissue, the additional electric current and electric power can be input. But because the penetrating humor is of small amount, the input electric power shortly enables humors to evaporate and roll-off may occur again soon. Therefore, the second ablation using conventional procedure cannot prominently enlarge the ablated area over 30 mm of diameter which the RTC system exhibits. The shape of ablated area also cannot be clearly changed. A few papers reported the results of double roll-off ablation procedure without change in probe positions,[20–22] showing that this double roll-off procedure cannot ablate the zone bigger than the diameter of the fully expanded needle. The ablation zone was approximately 3 cm with a 14-G LeVeen needle 35 mm in diameter.[20] Even with a 12-tine LeVeen needle 40 mm in diameter, the diameter perpendicular to the axis was 34.4 ± 2.1 mm and the axial diameter was 31.0 ± 6.2 mm.[21] The difference of energy between group 1 and group 2 is due to that of ablated volume because the required energy for ablation per volume is almost identical.[18]

We suggested in our previous study[18] that the smaller ablation zone produced by the conventional stepwise method was due to the facts that the hooks of the Super-Slim needles hardly extended to full extension during the slow insertion because the shaft was pushed back as the electrode was inserted toward the liver and that the tanned tumor or parenchymal tissues were removed from the surface of the multiple tines when they were once enclosed within the shaft in the new method, resulting in a better outcome of RF ablation. Our study identified another reason for the difference in the size of the ablated zone; the tines were extended separately in more cases of group 2, while some tines remained attached to each other in more cases of group 1 than of group 2. It is possible that this is because the tines gathered in one direction in the first step as the tip of the needle shaft was diagonally cut and the direction of the extension of each tine could not be reset in the conventional procedure. When all tines were separately extended, the cross-section was nearly circular and its

size was larger due to the better RFA, compared with the irregular shape and smaller size when two or three tines remained attached to each other. In addition, the median of the long axis with the new method is much larger not only than that with the conventional method using a slim needle but also that of the conventional method with an old needle of 15-G diameter.[3,13] It means this method using a slim needle is most appropriate when we want the largest ablated zone among various methods: the conventional method using a slim needle, that using a 15-G needle and the ablation using cool-tip needle.

In conclusion, the new extension procedure using the slim expandable needle allows coagulation of the largest area among various procedures using various types of needles. Additionally, the two kinds of stepwise procedures allow the selection of a more suitable procedure based on the tumor size and shape in each RFA.

REFERENCES

1 Bruix J, Sherman M. Management of hepatocellular carcinoma. *Hepatology* 2005; **42**: 1208–36.
2 Ikeda K, Kobayashi M, Saitoh S *et al.* Cost-effectiveness of radiofrequency ablation and surgical therapy for small hepatocellular carcinoma of 3 cm or less in diameter. *Hepatol Res* 2005; **33**: 241–9.
3 Mulier S, Ni Y, Miao Y *et al.* Size and geometry of hepatic radiofrequency lesions. *Eur J Surg Oncol* 2003; **29**: 867–78.
4 Livraghi T, Goldberg SN, Monti F *et al.* Saline-enhanced radio-frequency tissue ablation in the treatment of liver metastasis. *Radiology* 1997; **202**: 205–10.
5 Burdio F, Guemes A, Burdio JM *et al.* Large hepatic ablation with bipolar saline-enhanced radiofrequency: an experimental study in vivo porcine liver with a novel approach. *J Surg Res* 2003; **110**: 193–201.
6 Kurokohchi K, Watanabe S, Masaki T *et al.* Combined use of percutaneous ethanol injection and radiofrequency ablation for the effective treatment of hepatocellular carcinoma. *Int J Oncol* 2002; **21**: 841–6.
7 Watanabe S, Kurokohchi K, Masaki T *et al.* Enlargement of thermal ablation zone by the combination of ethanol injection and radiofrequency ablation in excised bovine liver. *Int J Oncol* 2004; **24**: 279–84.
8 Kurokohchi K, Masaki T, Miyauchi Y *et al.* Efficacy of combination therapies of percutaneous ethanol-lipiodol injection and radiofrequency ablation. *Int J Oncol* 2004; **25**: 1737–43.
9 Sugimoto K, Morimoto M, Shirato K *et al.* Radiofrequency ablation in a pig liver model: effect of transcatheter arterial embolization on coagulation diameter and histological characteristics. *Hepatol Res* 2002; **24**: 164–73.
10 Yamasaki T, Kurosawa F, Shirahashi H, Kusano N, Hironaka K, Okita K. Percutaneous radiofrequency abla-

tion therapy with combined angiography and computed tomography assistance for patients with hepatocellular carcinoma. *Cancer* 2001; **91**: 1342–8.

11 Kobayashi M, Ikeda K, Kawamura Y *et al.* Randomized controlled trial for the efficacy of hepatic arterial occlusion during radiofrequency ablation for small hepatocellular carcinoma-Direct ablative effects and a long-term outcome. *Liver Int* 2007; **27**: 353–9.

12 Chinn SB, Lee FT Jr, Kennedy GD *et al.* Effect of vascular occlusion on radiofrequency ablation of the liver. *AJR Am J Roentgenol* 2001; **176**: 789–95.

13 Kobayashi M, Ikeda K, Someya T *et al.* Stepwise hook extension technique for radiofrequency ablation therapy of hepatocellular carcinoma. *Oncology* 2002; **63**: 139–44.

14 Nakamuta M, Kohjima M, Morizono S *et al.* Comparison of tissue pressure and ablation time between LeVeen and cool-tip needle methods. *Comp Hepatol* 2006; **5**: 10.

15 Kotoh K, Nakamuta M, Morizono M *et al.* A multi-step, incremental expansion method for radio frequency ablation: optimization of the procedure to prevent increases in intra-tumor pressure and to reduce the ablation time. *Liver Int* 2005; **25**: 542–7.

16 Kotoh K, Enjoji M, Arimura E *et al.* Scattered and rapid intrahepatic recurrences after radio frequency ablation for hepatocellular carcinoma. *World J Gastroenterol* 2005; **11**: 6828–32.

17 Hirakawa M, Ikeda K, Kawamura Y *et al.* Lipiodol and dye at the site of ablation decreases during RFA. *Intervirology* 2008; **51**: 362–8.

18 Hirakawa M, Ikeda K, Kawamura Y *et al.* New ablation procedure for a radiofrequency liver tissue coagulation system using an expandable needle. *Liver Int* 2007; **28**: 214–9.

19 Yamashita T, Kaneko S. Treatment strategies for hepatocellular carcinoma in Japan. *Hepatol Res* 2012; (in press).

20 McGahan JP, Dodd GD 3rd. Radiofrequency ablation of the liver: current status. *AJR Am J Roentgenol* 2001; **176**: 3–16.

21 Pereira PL, Trubenbach J, Schenk M *et al.* Radiofrequency ablation: in vivo comparison of four commercially available devices in pig livers. *Radiology* 2004; **232**: 482–90.

22 Arata MA, Nisenbaum HL, Clark TW, Soulen MC. Percutaneous radiofrequency ablation of liver tumors with the LeVeen probe: is roll-off predictive of response? *J Vasc Interv Radiol* 2001; **12**: 455–8.

ORIGINAL ARTICLE—LIVER, PANCREAS, AND BILIARY TRACT

Clinical effectiveness of bipolar radiofrequency ablation for small liver cancers

Yukio Osaki · Kenji Ikeda · Namiki Izumi ·
Satoyoshi Yamashita · Hiromitsu Kumada ·
Shinji Hatta · Kiwamu Okita

Abstract

Background Radiofrequency ablation (RFA) is minimally invasive and can achieve a high rate of cure of liver cancer. This study was conducted to evaluate the efficacy and safety of a bipolar RFA device (CelonPOWER System) in the treatment of Japanese liver cancer patients.
Methods The study was a multicenter, single-group, open-label trial. The indications for RFA were based on the Japanese guidelines for the management of liver cancer. The subjects had a Child-Pugh classification of A or B, and the target tumors were defined as nodular, numbering up to 3 lesions, each of which was 3 cm or less in diameter, or solitary lesions up to 4 cm in diameter. To test for the non-inferiority of the CelonPOWER System, this system was compared with the Cool-tip RF System, which has already been approved in Japan, in terms of the complete necrosis rate (CNR).

Results The CNR obtained with the CelonPOWER System was 97.8 % (88/90 patients). The CNR obtained with the Cool-tip RF System was 86.2 % (50/58 patients), confirming the non-inferiority of the CelonPOWER System ($p < 0.001$, Fisher's exact test based on binomial distribution). Throughout the treatment and follow-up periods, there were no adverse events regarding safety that were uniquely related to the CelonPOWER System and there were no cases of device failure.
Conclusions The CelonPOWER System was confirmed to be an effective and safe RFA device. It could become extensively used as a safe next-generation RFA device, reducing the physical burden on patients.

Keywords Small hepatocellular carcinoma · Radiofrequency ablation (RFA) · Bipolar RFA · Conformite Europeenne (CE) mark · Non-inferiority to monopolar RFA

Y. Osaki
Department of Gastroenterology and Hepatology,
Osaka Red Cross Hospital, Osaka, Japan

K. Ikeda · H. Kumada
Department of Hepatology, Toranomon Hospital, Tokyo, Japan

N. Izumi
Division of Gastroenterology and Hepatology,
Musashino Red Cross Hospital, Tokyo, Japan

S. Yamashita · K. Okita (✉)
Department of Hepatology, Center for Liver Disease,
Social Insurance Alliance Shimonoseki Kohsei Hospital,
Kami-Shinchi Cho 3-3-8, Shimonoseki,
Yamaguchi 750-0061, Japan
e-mail: k.okita@kousei-h.jp; k.okita@www.kousei-h.jp

S. Hatta
Olympus Medical Systems Corp, Tokyo, Japan

Introduction

According to a report of the Japanese Ministry of Health, Labor and Welfare in 2010, the number of deaths due to malignancies, including hepatocellular carcinoma (HCC), which is the most common type of primary liver cancer, has tended to increase annually [1]. In the 2007 report of the Japanese Ministry of Health, Labor and Welfare, the mortality of liver cancer was the 3rd highest among malignant diseases, following gastric cancer and lung cancer [2]. HCC appears in cirrhotic liver, and cirrhotic liver often results from alcohol abuse or chronic hepatitis B virus (HBV) or HCV infection. The presence of liver cirrhosis limits HCC treatment options, because surgery and systemic chemotherapy impair residual liver function and can induce fatal liver failure. In addition,

even if the primary tumor is completely resected, there is a very high recurrence rate in the residual liver [3, 4].

Radiofrequency ablation (RFA) is a minimally invasive method that can yield radical localized therapeutic results, and it has become a standard treatment for small liver cancers 3 cm or less in diameter [5].

Three different RFA systems have been introduced in Japan, all consisting of monopolar devices. One of the main problems with monopolar RFA devices is that the electrical current flows between the electrodes and the grounding pad that is used in these devices. The current flows in a wide area of the body, which may cause systemic symptoms, such as heat retention and perspiration. In addition, because the applicator is distant from the grounding pad, its low energy efficiency requires a long ablation time. Moreover, energy concentration can occur owing to an unanticipated current pathway between the applicator and grounding pad, posing a risk of burns at the grounding pad patch site and at non-treatment sites [3, 6–9].

A bipolar system, in contrast to the monopolar systems, features as its principal characteristic an electrical current flowing between two electrodes on a single probe. With a bipolar system, the current pathway is limited to only within the treatment area, thus eliminating the need for a grounding pad. A bipolar RFA system also overcomes such disadvantages of a monopolar system as the occurrence of heat retention and other side effects, low energy efficacy, and thermal injuries at electrode pad sites caused by an electrical current flowing in the body. The simultaneous use of multiple applicators with a bipolar system makes it possible to achieve a sufficiently large thermocoagulation volume with a single ablation procedure. That is, one ablation is usually sufficient for a wide area and this enables a short ablation time. In addition, ablation can be achieved even if the electrodes are not inserted directly into the tumor. The use of the bipolar system with multiple applicators with a wide ablation area maximizes the effectiveness of the bipolar system.

The purpose of this study was to evaluate the safety and efficacy of a bipolar RFA device, the CelonPOWER System, in order to obtain the clinical data necessary for an application for its regulatory approval in Japan. The study and protocol were designed in compliance with Japanese good clinical practice (GCP) based on the advice from the Pharmaceuticals and Medical Devices Agency (PMDA) of the Japanese regulatory authority. In designing this study, we were requested by the PMDA to compare this device with an existing RFA device (that had been already approved in Japan) and we selected the data from the 2002 to 2003 clinical study of the Cool-tip RF System as valid control data. The study of the Cool-tip RF System was also conducted to obtain marketing approval in Japan [10]. This study was sponsored by Olympus Medical Systems Corp.

Patients, materials, and methods

Device

Celon AG Medical Instruments (Teltow, Germany) developed a bipolar RFA device (CelonPOWER System) in order to overcome the disadvantages of monopolar RFA devices. Unlike a monopolar RFA system, the prime characteristic of this new device is its bipolar feature, i.e., two electrodes are located on the same needle (Fig. 1a, b), allowing electricity flow only between the electrodes at the treatment target site, eliminating both the need for a grounding pad and the danger of burns (Fig. 2a, b).

The bipolar characteristics of the CelonPOWER system ensure the return of power to the device, and the simultaneous use of multiple applicators yields an extensive ablated area in a single treatment, which can reduce treatment time and the burden on the patient. This eliminates the need for repeated reinsertion of single monopolar needles to perform overlapping ablation. Another advantage of the bipolar device is that electric current is immediately retrieved, preventing it from flowing to unintended sites. The CelonPOWER System was awarded the Conformite Europeenne (CE) mark in 2003, and since then its use has spread mainly in Europe [11–17].

The CelonPOWER System consists of a high-frequency power generator, a water pump, and computerized applicators for regulation of the current frequency. The basic
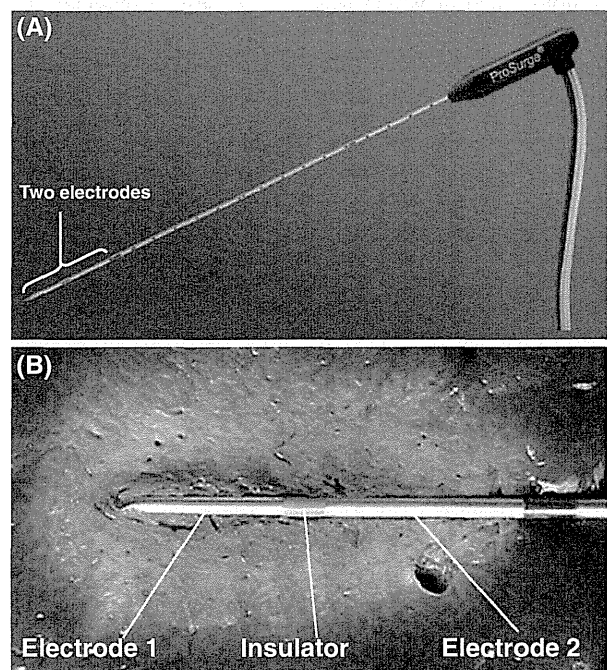

Fig. 1 In the CelonPOWER System, each applicator is needle-shaped and has two electrodes near its tip
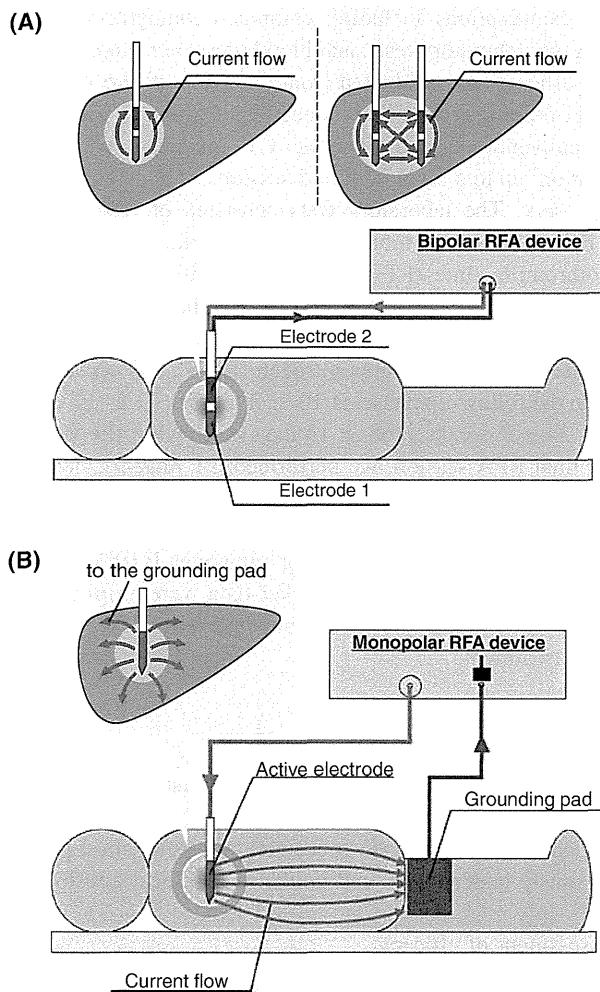
(A)

(B)

Fig. 2 Differences in the electrical flow routes of **a** the monopolar and **b** the bipolar (CelonPOWER System) radiofrequency ablation (*RFA*) systems. With the bipolar system (CelonPOWER System), the electrical current flows between the two electrodes, and for this reason the current pathway is limited to the treatment area, allowing lower power to be concentrated in a specific area and yet yielding effects equivalent to those obtained by higher energy monopolar devices, the power of which is dispersed throughout the body to the dispersion grounding pads placed under the patient

frequency of the power generator is 470 kHz, with a maximum output of 250 W. All the needles for RFA are 1.8 mm in width (15 G) but there are 3 different lengths: 20, 30, and 40 mm. The Cool-tip RF System needles are 1.5 mm in width (17 G).

Bipolar applicators

Each applicator is needle-shaped and has two electrodes near its tip. The electrical current flows between the two electrodes on the single probe, limiting the current pathway to within the treatment area. A grounding pad is

unnecessary (Fig. 2a). The applicators are cooled by the internal circulation of chilled water.

Multipolar application

When simultaneously using multiple applicators (up to 3 can be employed simultaneously), it is possible to treat relatively large cancers that could not be sufficiently ablated by means of one insertion of a single applicator. The high-frequency electrical current flows sequentially between the electrodes of the applicators (6 electrode pair combinations when there are 2 applicators, 15 electrode combinations when there are 3 applicators) (Fig. 3a).

Resistance controlled automatic power (RCAP)

RCAP is a function that monitors the change of electric resistance between the electrodes, and automatically
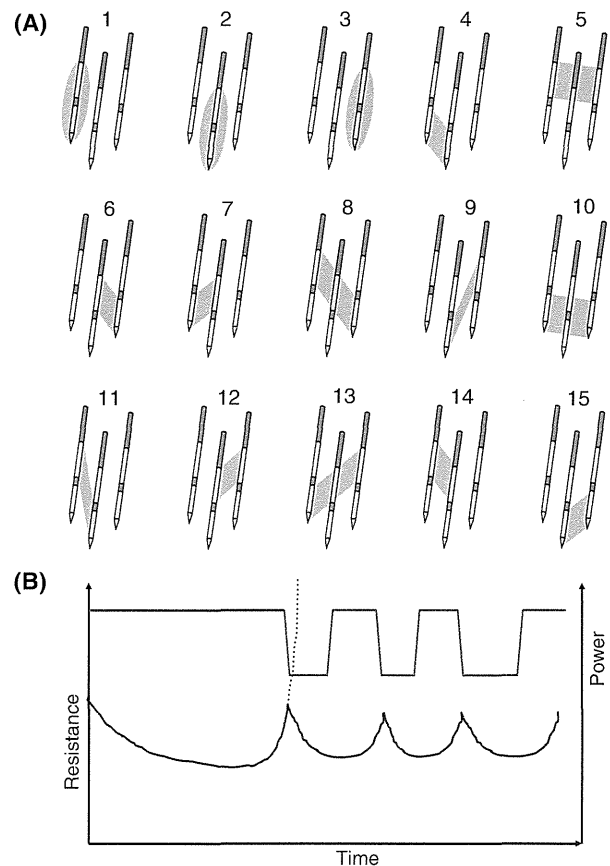
(A)

(B)

Fig. 3 When 3 applicators are employed, the high-frequency electrical current flows sequentially between 15 combinations of electrode pairs (**a**), and an image is generated of the automated control of the output by the resistance controlled automatic power (RCAP) function (**b**). RCAP is a function by which the degree of change in the electrical resistance among the electrodes (increase/decrease in slope) is monitored, and the high-frequency power output is automatically controlled

controls the high-frequency power (Fig. 3b). This function makes it possible to prevent unexpected rapid increases in electrical resistance resulting from tissue necrotization.

Patients

This clinical study was carried out based on the HCC treatment algorithm in the Scientific Data-based Clinical Practice Guidelines for Liver Cancer-2005 Version [18]. We enrolled adult male and female patients aged 20 years or older with primary or metastatic small liver cancers who had provided written informed consent. Target tumors were defined as nodular, numbering up to 3 lesions, each of which was 3 cm or less in diameter, or solitary lesions up to 4 cm in diameter. Exclusion criteria included a Child-Pugh grade of C, or platelet count below 50000/μl. Informed consent was obtained from 104 patients, of whom 96 were initially enrolled, but 5 withdrew consent before the trial started. The trial was therefore carried out in a total of 91 patients (112 treated lesions) with intention-to-treat (ITT) analysis, and 90 patients were eligible for the analysis of efficacy.

Patient details

Table 1 summarizes the data on the background characteristics of the 91 patients and 112 treated lesions treated in the study (73 patients had 1 lesion, 15 had 2, and 3 patients had 3 lesions; Table 1). The cohort consisted of 61 men and 30 women, and the mean age (±SD) was 69 ± 10 years; 84 patients had primary liver cancer, while 7 had metastatic liver cancer.

Study design

This prospective multicenter, collaborative, single-group, open-label study was conducted at 5 institutions between December 2008 and December 2009. The study protocol was approved by each center's institutional review board. The trial treatment period lasted from the acquisition of written informed consent through completion of the final treatment (maximum 3 treatments), in addition to a follow-up period from the day after the final examinations of the treatment period until the completion of examinations performed 24 weeks later. The non-inferiority of the CelonPOWER System was evaluated relative to the results obtained with a Cool-tip RF System in 2002–2003 [10].

Study methodology

Figure 4 shows the study procedures. During the treatment period, the following procedures were performed, in the order listed: registration of eligible patients, RFA treatment and examinations including computed tomography (CT) imaging, laboratory tests, and blood pressure measurement. The efficacy was evaluated from the extent of the necrotic area (tumor necrosis; TN) induced by ablation as measured on conventional and dynamic CT imaging. Additional ablation, up to a maximum of 3 sessions, was performed as necessary. The laboratory tests consisted of RBC count, WBC count, hemoglobin level, hematocrit, platelet count, prothrombin time (PT) activity, total bilirubin, albumin, aspartate aminotransferase (AST), alanine aminotransferase (ALT), alkaline phosphatase (ALP), lactate dehydrogenase (LDH), blood urea nitrogen (BUN), and creatinine.

In the follow-up phase, at 10 ± 2 weeks (70 ± 14 days) and 24 ± 2 weeks (168 ± 14 days) following the day of the final RFA session, we performed CT imaging, laboratory tests, blood pressure measurement, measurement of alpha-fetoprotein (AFP), and measurement of protein induced by vitamin K absence or antagonist II (PIVKA-II). The CT images and tumor marker data were employed to assess the continuity of the therapeutic effect (TE) of the RFA treatment.

RFA procedure

The procedure with the CelonPOWER System device was similar to the procedure with the existing monopolar RFA devices. In all cases, the procedure was performed percutaneously under ultrasound guidance and local anesthesia.

Assessment of efficacy

TN was assessed using 5 grades, in accordance with the Criteria for Direct Effects of Liver Cancer Treatment (1994) [19]. Class V tumor necrosis (100 % TN) of liver cancer following the final RFA session was defined as "complete necrosis," and the percentage of patients achieving Class V TN was defined as the "complete necrosis rate" (CNR), the primary endpoint. The TN classification was used for short-term (during treatment) evaluation, and this was the only evaluation reported for the Cool-tip RF System in the marketing authorization holder's application for Japanese government approval. However, now the government demands not only short-term evaluation, but also long-term evaluation, for which such parameters as TE, overall response, and complete response (CR) are used.

The secondary endpoints of our study were the number of RFA sessions, the TE, and the overall assessment of the TE. The assessment of the immediate TE and the overall assessment of TE were performed in accordance with the General Rules for the Clinical and Pathological Study of Primary Liver Cancer (2008) [20]. The TE was classified as either CR (total necrosis and normalization of all tumor

Table 1 Patient background factors and lesion characteristics

Patients (n = 91)		Lesions (n = 112)	
Background factors	N (%)	Characteristics	N
Sex		Maximum dimension (cm)	
M	61 (67.0)	<1.0	22
F	30 (33.0)	1.1–2.0	69
Age (years)		2.1–3.0	17
31–40	1 (1.1)	3.1–4.0	4
41–50	4 (4.4)	Mean ± SD	
51–60	9 (9.9)	1.6 ± 0.7	
61–70	32 (35.2)	Subsegment	
71–80	34 (37.4)	S1	0
81–90	11 (12.1)	S2	6
Cancer		S3	9
Primary	84 (92.3)	S4	8
Metastatic	7 (7.7)	S5	18
Underlying disease		S6	20
Cirrhosis	63 (69.2)	S7	18
Chronic hepatitis	22 (24.2)	S8	33
None	6 (6.6)		
Child-Pugh classification			
Grade A	83 (91.2)		
Grade B	8 (8.8)		
Number of treated lesions			
1	73 (80.2)		
2	15 (16.5)		
3	3 (3.3)		
Previous treatment of primary disease			
Yes	40 (44.0)		
No	51 (56.0)		

markers), or others. In addition, ITT analysis was performed in regard to the cumulative local recurrence rate and the overall assessment of the TE.

Assessment of safety

The following safety endpoints were assessed in all 91 patients in whom the study was conducted: overall safety assessment, adverse events, device-related adverse events, device failure, laboratory test values, and blood pressure.

Statistical analysis

Statistical analysis was performed using a one-sided significance level of 2.5 % for the primary endpoint. In principle, a two-sided significance level of 5 % was used for the other endpoints to avoid data dispersion. The CNR (the primary endpoint) was calculated as the percentage of the total number of patients who achieved Class V TN, and its exact one-sided 97.5 % confidence

interval was calculated. For the secondary endpoints, the variables and their ratios were compiled, and the basic statistics for the mean and standard deviation were calculated.

Results

Patients

Written informed consent was obtained from 104 patients, including the 96 patients in the study. The study was conducted in 91 of these patients, and treatment was completed in 90 patients. Eighty-eight of the 90 patients (excluding 2 TN4 patients) were followed up. Five patients discontinued the study during the follow-up period, leaving 83 patients who completed the follow-up period. Three patients were excluded because of unacceptable enrollment dates, so the final number of patients eligible for the efficacy analysis was 80.

Fig. 4 Clinical study procedure. *TN* Tumor necrosis
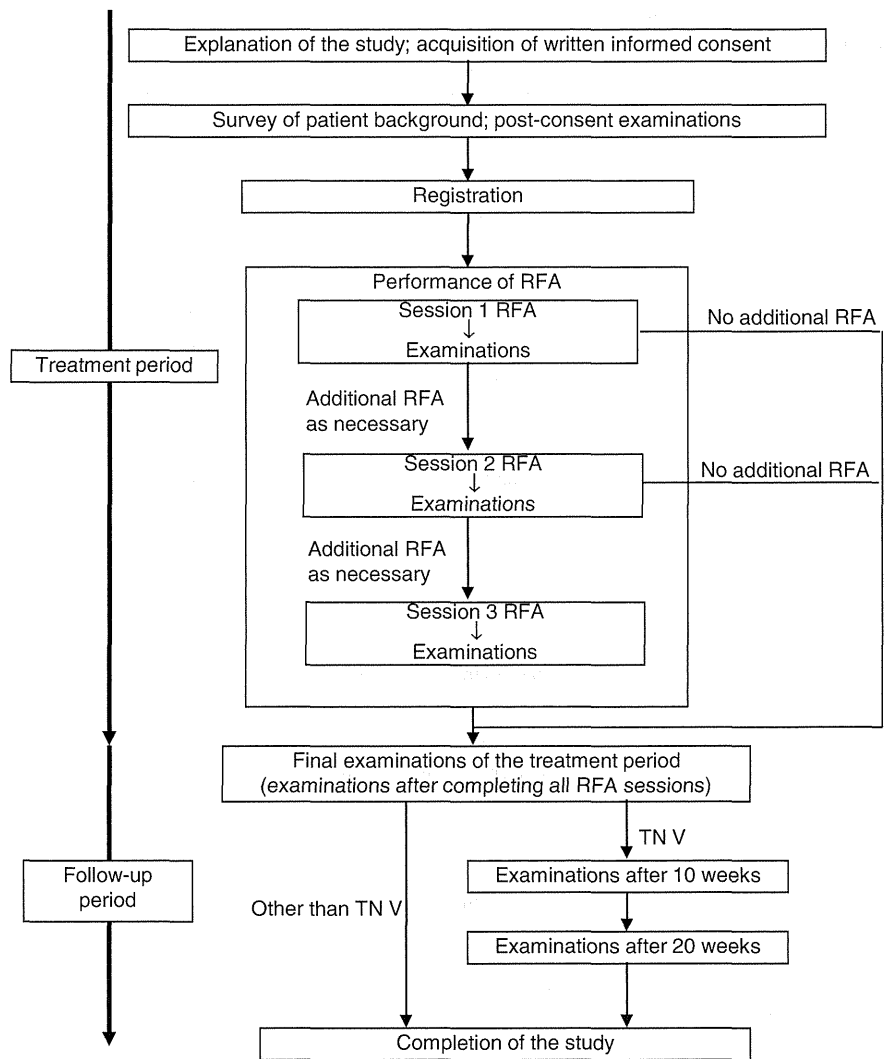
Efficacy

Of the 90 patients who completed this clinical treatment study, 88 showed Class V TN (97.8 %). The 2 patients (2.2 %) who did not show 100 % TN both had primary liver cancers and were categorized as Class IV TN. The CNR was 100 % in patients with metastatic liver cancer (7/7 patients) and 97.6 % in patients with primary liver cancer (81/83 patients). The Japanese package insert for the Cool-tip RF System [21] states that the CNR obtained by that system was 86.2 % (50/58 patients). Assuming a 5 % non-inferiority margin, the lower limit of the confidence interval (one-sided 97.5 %) was 92.2 %, and the p value was <0.001 for the exact test based on binomial distribution.

The initial success rate (Class V TN after 1 session) was 77.8 % (70 of 90 patients), while Class V TN was seen in 16 (17.8 %) patients following a second session. The remaining 4 (4.4 %) patients underwent a third RFA

session, and 2 were rated as Class V TN following that session.

We used 1 applicator in 20 patients, 2 simultaneously in 54 patients, and 3 simultaneously in 16 patients. We used 30-mm electrodes in all the patients, except in 3 of the 16 patients in whom 3 electrodes were used simultaneously; in these 3 patients we used 3 40-mm electrodes. A representative case in which 3 applicators were used is shown in Fig. 5.

Of the 88 patients who proceeded to the follow-up phase, excluding the single out-of-hospital fatality, examination at 24 weeks showed that CR was obtained in 94.3 % (82/87). The cumulative local recurrence rate at the end of 24 weeks in the follow-up period was 5.7 % (5/87 patients; ITT analysis) (Table 2).

Figure 6a, b shows a comparison of the treatment results of the Cool-tip RF System clinical trial [21] and the number of patients analyzed for the CNR and the efficacy